MICROWAVE CHARACTERIZATION OF PARYLENE C DIELECTRIC AND BARRIER PROPERTIES

Nikolas D. Barrera[1], Jacob T. Pawlik[2], Eugene J. Yoon[1], James C. Booth[2], Christian J. Long[2], Nathan D. Orloff[2], Ellis Meng[1], and Angela C. Stelson[2]

[1]Alfred E. Mann Department of Biomedical Engineering, University of Southern California, USA

[2]RF Technology Division, National Institute of Standards and Technology, USA

ABSTRACT

Parylene C thin films are commonly used as a passivation layer, protective coating, or substrate material in implantable medical devices. However, fluid or vapor may permeate through Parylene C films over time through defects, film edges, or bulk diffusion and lead to device failure *in vivo*. Such failure can be difficult to detect using electrochemical impedance spectroscopy (0.1 Hz – 1 MHz) which does not capture the dielectric contributions of fluid at higher frequencies.

We present a method for tracking broadband (1 MHz – 110 GHz) microwave dielectric properties of polymer-fluid interfaces. Using 2D electromagnetic modeling, we simulated measurement sensitivity to potential changes in Parylene C film dielectric properties and estimated sensitivity to changes in film relative permittivity as small as ±0.1 and fluid layers under films as small as 5 nm. Results were used to aid in the interpretation of measurements of soaked Parylene C films. These results are informative development of robust, hermetic polymer films in implantable medical devices and other RF applications in the analysis of complex fluids.

KEYWORDS

Parylene C, Thin film, Broadband, Microwave, Dielectric, Spectroscopy, Interfaces, Microfluidic

INTRODUCTION

Parylene C is used as a barrier and insulation material in medical implants because it is biocompatible, flexible, and coats conformally [1]. Parylene C is a popular substrate material in thin film implants because it is compatible with microfabrication processes [2]. However, the barrier properties of Parylene thin films may degrade within months *in vivo* [3], leading to electrical shorting and device failure. Contributing mechanisms may include film oxidation, poor film adhesion or delamination, and fluid permeation or diffusion.

Many studies have examined the dielectric and barrier properties of Parylene C films *in vitro* via electrochemical impedance spectroscopy (EIS) [4][5]. However, EIS is limited to frequencies (in the range of 0.1 Hz – 1 MHz) and is unable to capture phenomena that occur at higher frequencies, particularly dipolar relaxations, and ionic conduction. Wireless medical devices often employ radio-frequency data or power transfer, typically via transmission through biological tissue. At these frequencies, dipolar relaxations and ionic conduction contribute to dielectric loss, which causes signal attenuation and undesired tissue heating.

In contrast, microwave microfluidic spectroscopy (MMS), utilizes a broader range of frequencies (40 kHz – 110 GHz) that can capture multiple physical phenomena, such as electric double layer formation, ionic conduction, ion pairing, and dipolar relaxation [6]. MMS measures complex scattering-parameters (S-parameters) of coplanar waveguides (CPWs) coupled with microfluidic structures. CPWs provide a simple geometry to carry high frequency signals [7], and the S-parameter data can be fit to a transmission line model from which dielectric properties can be extracted.

The broadband properties of Parylene C-coated CPWs after long-term exposure to water or ionic fluid were measured using MMS in our previous work [8]. However, mapping S-parameters to physical changes in the films was unclear. Previously, we evaluated the fit of MMS measurements to a transmission line model. In this study, we extended on this capability and performed parametric simulations to quantify the sensitivity of MMS to potential physical changes in the Parylene C film from fluid exposure, such as delamination, fluid intrusion, film swelling, and shifts in film permittivity. Parametric simulation results were used to aid interpretation of measured S-parameters and determine if any significant changes in film dielectric properties were induced by fluid exposure. Discerning the true physical changes is crucial in identifying failure mechanisms and informing mitigation strategies to achieve robust polymer films for implantable medical devices.

MATERIALS AND METHODS

Fabrication

We fabricated Parylene C-coated platinum CPWs as in [9] on a fused silica wafer via a metal lift-off followed by chemical vapor deposition of Parylene C. We fabricated reference wafers with gold CPWs to calibrate S-parameters to the probe tips of the vector network analyzer (VNA) probes. We cast a polydimethylsiloxane (PDMS) microfluidic cover in a 3D-printed mold and integrated the cover on CPWs for MMS (Fig. 1a, b.)

Measurement

We obtained S-parameter measurements (100 MHz – 110 GHz) using a VNA and were calibrated with multiline thru-reflect-line (TRL) and series resistor calibrations [12], leaving only the section shown in Fig. 1c as the device-under-test. Total measurement uncertainty was determined by compounding Type A and B uncertainties by a sum of root mean squares [8].

Measurements from our previous study [8] were used for analysis in this study. CPWs were soaked over 2 months in either deionized (DI) water at 20°C, 1×PBS (phosphate-

buffered saline) at 20°C, or 1×PBS at 37°C. The change in measured S-parameters following soaking were used to assess changes in film dielectric properties. Measured results were compared to simulated results.

Simulation

We performed 2D electromagnetic simulations to model the broadband properties of the CPW microfluidic assembly (Fig. 1d). The assembly sections are defined in Fig. 2. Using the measured geometry and material properties (Table 1), we simulated the 2D electric field at the microfluidic channel to assess the contribution of the Parylene C film to the effective dielectric properties.

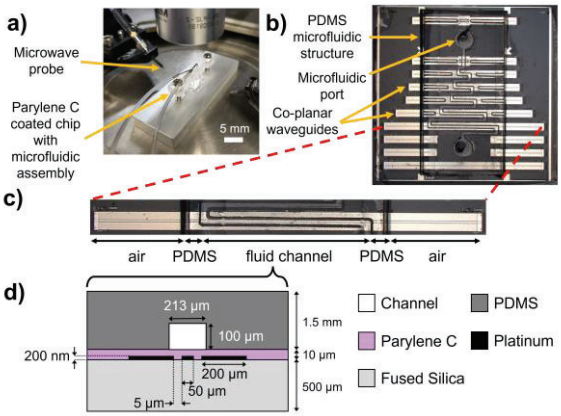

Figure 1: Measurement set-up of Parylene C coated CPW microfluidic assembly [8]. a) CPW with PDMS microfluidic assembly on the probe station. b) Top-down view of the assembly. c) Top-down view of a single coplanar waveguide (4.16 mm length). d) Illustrated cross-section at microfluidic channel with dimensions.

A dual Debye relaxation model (Eqn. 1) [9] was selected for DI water [10] and a Cole-Cole model (Eqn. 2) of 0.9% saline [11] for 1×PBS:

$$\epsilon_D(\omega) = \epsilon_\infty + \frac{\epsilon_s - \epsilon_2}{1+i\omega\tau_2} + \frac{\epsilon_2 - \epsilon_\infty}{1+i\omega\tau_2} \quad (1)$$

$$\epsilon_C(\omega) = \epsilon_\infty + \frac{\epsilon_s - \epsilon_\infty}{(1+i\omega\tau_1)^{1-\alpha}} \quad (2)$$

where ϵ_s, ϵ_2, and ϵ_∞ are the low, intermediate, and high frequency permittivity values, respectively, τ_1 and τ_2 are relaxation time constants, ω is the angular frequency, and α is a factor of symmetrical broadening of the relaxation peak.

The fit of our measurements to a transmission line model was previously demonstrated by comparing simulated to measured S-parameters [8]. Similarly, we obtained transmission line circuit model elements R_i, L_i, C_i, and G_i for each section i in Fig. 2 from simulations. Then we computed each section's characteristic impedance Z_i and propagation constant γ_i [13]:

$$Z_i = \frac{\sqrt{R_i + i\omega L_i}}{\sqrt{G_i + i\omega C_i}} \quad (3)$$

$$\gamma_i = \sqrt{(R_i + i\omega L_i)(G_i + i\omega C_i)} \quad (4)$$

Table 1: Material properties for simulated CPWs.

Material	$\epsilon(\omega)$	σ (S/m)
Silica	3.82	0
Platinum	1.00	0.90×10^7
Parylene C	3.00	0
PDMS	2.77	0
DI H_2O	*Eqn.* (1)[10]	0
1×PBS	*Eqn.* (2)[11]	1.60

Using Z_i and γ_i, we derived the transmission parameter matrix T_i and the impedance transformers $Q_{Z_m}^{Z_n}$ for each transition of Z_i between sections:

$$T_i = \begin{bmatrix} e^{-\gamma_i l_i} & 0 \\ 0 & e^{\gamma_i l_i} \end{bmatrix} \quad (5)$$

$$Q_{Z_m}^{Z_n} = \frac{1}{2Z_m}\left|\frac{Z_m}{Z_n}\right|\sqrt{\frac{Re(Z_n)}{Re(Z_m)}}\begin{pmatrix} Z_n + Z_m & Z_n - Z_m \\ Z_n - Z_m & Z_n + Z_m \end{pmatrix} \quad (6)$$

where n and m denote transmission of a signal from section n to section m. Then we computed a T-matrix T_{all} representing the entire device in Fig. 2a, corrected to 50 Ω by cascading the T-matrices:

$$T_{all} = Q_1^{50\Omega} T_1 Q_2^1 T_2 Q_3^2 T_3 Q_4^3 T_4 Q_3^4 T_3 Q_2^3 T_2 Q_1^2 T_1 Q_{50\Omega}^1 \quad (7)$$

where indices of each matrix correspond to section numbers in Fig. 2a. We converted T-matrices directly to S-parameters that model the CPW assembly in Fig. 1.

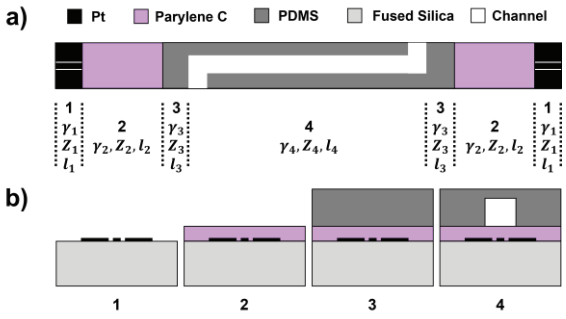

Figure 2: Diagram of each section of the CPW microfluidic assembly [8]. a) Top-down view of each section i with transmission line model quantities γ_i and Z_i, and line lengths l_i. b) Cross-section of each section i.

Parametric simulations were used on simplified model systems to assess the sensitivity of measured S-parameters to potential physical changes from fluid, including delamination, fluid intrusion, film swelling, and shifts in film permittivity (Fig. 3). Parylene film permittivity ($\epsilon_{Parylene}$) was varied from 2.5 to 3.5. The thickness of DI water (h_{H2O}), and PBS (h_{PBS}) were varied from 0.001 µm to 0.025 µm and represent delamination from fluid. Similarly, the thickness of an air layer (h_{air}) was varied from 0.01 µm to 1 µm to represent film delamination without fluid. Film thickness (h_{film}) was varied from 0.01 µm to 10 µm to represent film swelling.

The linear magnitude of the S-parameters ($|S_{11}|$ and $|S_{21}|$) were used for computation to emphasize minute changes from parameter variation. The sensitivity to each parameter was evaluated by computing the change in broadband S-parameter magnitude:

$$\Delta|S| = |S|_i - |S|_0 \quad (8)$$

where $|S|_i$ are the broadband linear magnitude S-parameters resulting from a parameter value i and $|S|_0$ are the broadband linear magnitude S-parameters prior to any imposed conditions.

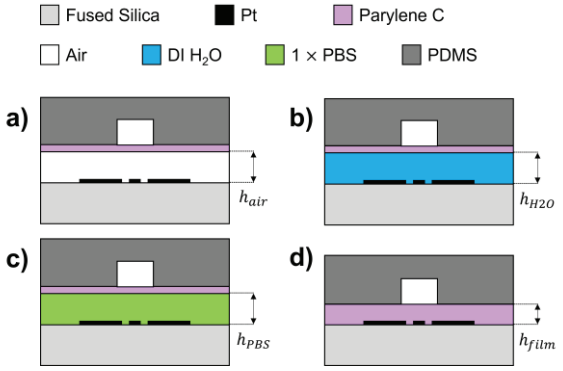

Figure 3: Parametric simulation model systems for S-parameter sensitivity to physical changes in the Parylene C film at the microfluidic channel. Uniform, progressive delamination of Parylene C with a) air, b) DI H_2O, or c) 1×PBS underneath the film. D) Uniform film swelling.

RESULTS AND DISCUSSION

The simulated electric field distributions in Fig. 4 correspond to the film parameters in Fig. 3. In Fig. 4a, the air layer results in a more broadly distributed electric field above the CPW due to the lower effective permittivity relative to the substrate. In Fig. 4b and 4c, the electric field is more tightly confined, likely due to the greater permittivity and additional dielectric loss contributed by the fluid layers.

The sensitivity of S-parameters to changes in the individual parameters of interest are shown in Fig. 5. Typical measurement uncertainty from measurements in [8] for S_{11} and S_{21} are overlaid in Fig. 5. The uncertainty varies across frequency and is minimal at around 5 to 9 GHz, primarily contributed from sources of Type A uncertainty. Changes in S-parameters at these frequencies are less likely to be compounded with measurement error and are thus more sensitive to true, dielectric changes in the film.

MMS was sensitive to a change in $\epsilon_{Parylene}$ as small as ±0.1, where S_{21} at 6 GHz exceeded the measurement uncertainty (Fig. 5). In Fig. 5b, delamination with h_{air} as small as 10 to 50 nm yielded comparable results for S_{21} at 6 GHz. Sensitivity was greater when fluid was introduced (Fig. 5c, d), fluid layer thicknesses h_{H2O} and h_{PBS} as small as 1 to 5 nm resulted in a change in S_{21} greater than the measurement uncertainty. Additionally, there is a unique, low-frequency dependence with PBS layer thickness, due to ionic conductivity. S-parameters in Fig. 5e was less sensitive to changes in film thickness and required an increase of at least 1 µm in film thickness h_{film} to exceed measurement uncertainty.

Measured changes in S-parameters of Parylene C CPWs exposed to DI H_2O and 1×PBS over 2 months from [8] is shown in Fig. 5f, for direct comparison to sensitivity to each parameter of interest. For DI H_2O and 1×PBS at 20°C, the change remained within the bounds of measurement uncertainty, suggesting no measurable change in the geometry or dielectric properties of the Parylene C film. For the film exposed to 1×PBS at 37°C, there was a slight change in S-parameters that exceeds the uncertainty at 5 to 9 GHz. Comparing this change to the simulated results in Fig. 5a-e suggests a significant change in effective permittivity. The slight vertical shift at 100 MHz to 1 GHz for 1×PBS in Fig. 5f may be indicative of an ionic conductivity as seen in Fig. 5d, suggesting there is likely an ingress of 1×PBS. Discerning the exact physical changes in the film requires additional characterization.

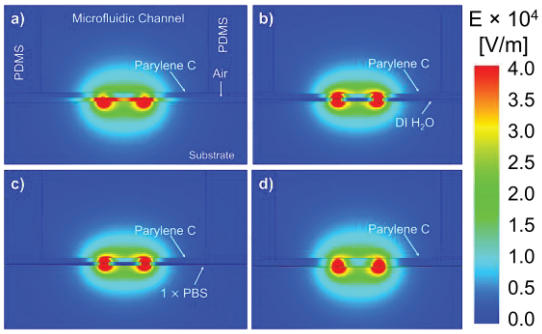

Figure 4: Parametric simulation electric field distributions at the microfluidic channel for a) h_{air}, b) h_{H2O}, c) h_{PBS}, d) and h_{film}. The intensity of the electric field generated by the CPW is given as a gradient scale on the right.

In each case, sensitivity could be enhanced with further calibration as the S-parameters include redundant contributions from non-channel sections of the CPW. Sensitivity was greatest with the introduction of fluid, due to the large mismatch in dielectric properties between fluid and Parylene C or air. However, it is unknown how the dielectric properties of the film change from fluid present in the film matrix. Furthermore, shifts in film geometry will likely be more complex and non-uniform. Future experiments could validate whether the estimated sensitivity to each parameter is accurate, however replicating changes such as delamination in the film in a controlled, physical experiment is challenging. Direct measurement of sensitivity would introduce uncertainty with each measurement and would result in lower sensitivity than estimated here.

CONCLUSION

We evaluated a method for measuring microwave-frequency dielectric properties of polymer-fluid interfaces. We estimated the measurement sensitivity to changes in relative permittivity as small as ±0.1 or fluid layers as thin as 5 nm through parametric simulations. Simulation results were used to aid interpretation of previous measurements of Parylene C films soaked in DI water and 1×PBS. In future applications of our method, such as characterizing other polymer-fluid interfaces, we suggest performing a similar parametric analysis of sensitivity. Our results demonstrate our method is an effective technique for measuring and modeling microwave dielectric properties of polymer-fluid interfaces Overall, our results are valuable

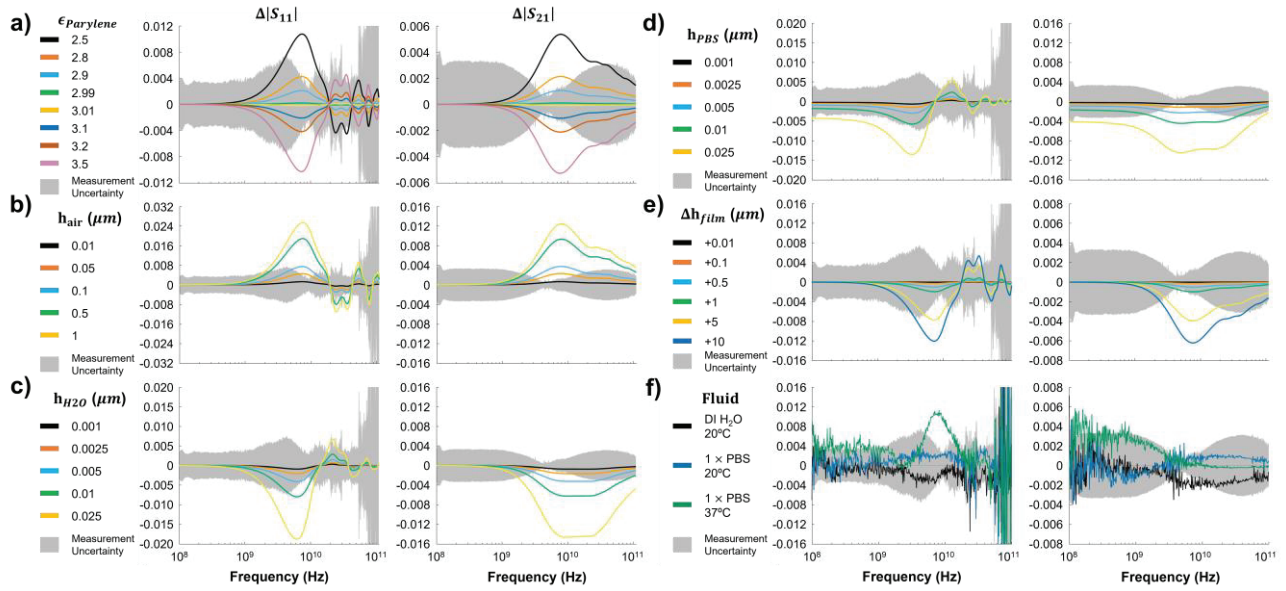

Figure 5: Simulated broadband sensitivity of S -parameter magnitude to a) Parylene C permittivity, b) delamination (air underneath), c) DI H_2O accumulation under film, d) 1×PBS accumulation under film, and e) film swelling. f) Measured changes in broadband S-parameters following soaking in several fluid soaking conditions [8]. Typical measurement uncertainty prior to soaking is overlaid in each case.

for the development of robust, wireless devices in fluid media such as implantable medical devices.

ACKNOWLEDGEMENTS

This work was supported in part by the NSF under the INTERN supplement affiliated with Award IIP-1827773. The content of the information does not necessarily reflect the position or the policy of the U.S. federal government, and no official endorsement should be inferred. Usage of commercial products herein is for information only; it does not imply recommendation or endorsement by NIST.

REFERENCES

[1] M. Golda-Cepa, K. Engvall, M. Hakkarainen, A. Kotarba, "Recent progress on parylene C polymer for biomedical applications: A review," *Progress in Organic Coatings*, vol. 140, 2020.

[2] B. J. Kim, E. Meng, "Micromachining of Parylene C for bioMEMS", *Polymers for Advanced Technologies*, vol. 27, no. 5, pp. 564–576, 2016.

[3] A. Lecomte, A. Degache, E. Descamps, L. Dahan, C. Bergaud, "In vitro and in vivo biostability assessment of chronically-implanted Parylene C neural sensors," *Sens Actuators B Chem*, vol. 251, pp. 1001–1008, 2017.

[4] W. Chun, N. Chou, S. Cho, S. Yang, and S. Kim, "Evaluation of sub-micrometer parylene C films as an insulation layer using electrochemical impedance spectroscopy," *Prog Org Coat*, vol. 77, no. 2, pp. 537–547, Feb. 2014.

[5] P. Takmakov, K. Ruda, K. Scott Phillips, I. S. Isayeva, V. Krauthamer, and C. G. Welle, "Rapid evaluation of the durability of cortical neural implants using accelerated aging with reactive oxygen species," *J Neural Eng*, vol. 12, no. 2, 2015.

[6] C. A. E. Little, N. D. Orloff, I. E. Hanemann, C. J. Long, V. M. Bright, and J. C. Booth, "Modeling electrical double-layer effects for microfluidic impedance spectroscopy from 100 kHz to 110 GHz", *Lab on a Chip*, vol. 17, no. 15, pp. 2674–2681, 2017.

[7] D. M. Pozar, "Transmission Lines and Waveguides," in *Microwave engineering*, 4th ed., Hoboken: Wiley, 2012, p. 189.

[8] J. T. Pawlik, N. D. Barrera, E. Yoon, J. Booth, C. Long, N. Orloff, E. Meng, A. Stelson, "The influence of water and ion permeation on Parylene C film properties", *IEEE Journal of Electromagnetics, RF and Microwaves in Medicine and Biology* (submitted, under review).

[9] E. Yoon, A. Stelson, N. Orloff, C. Long, J. Booth, and E. Meng, "The effect of annealing thin film Parylene C-platinum interfaces characterized by broadband dielectric spectroscopy", in *21st International Conference on Solid-State Sensors, Actuators and Microsystems,* Jun. 2021, pp. 884–887.

[10] R. Buchner, J. Barthel, and J. Stauber, "The dielectric relaxation of water between 08C and 358C," 1999.

[11] P. D. Jensen, P. M. Meaney, N. R. Epstien, and K. D. Paulsen, "Cole-Cole parameter characterization of urea and potassium for improving dialysis treatment assessment," *IEEE Antennas Wirel Propag Lett*, vol. 11, pp. 1598–1601, 2012.

[12] X. Ma *et al.*, "A Multistate Single-Connection Calibration for Microwave Microfluidics," *IEEE Trans Microw Theory Tech*, pp. 1–9, 2017.

[13] W. Heinrich, "Quasi-TEM description of MMIC coplanar lines including conductor-loss effects", *IEEE Transactions on Microwave Theory and Techniques*, vol. 41, no. 1, pp. 45–52, 1993.

CONTACT

*E. Meng, tel: +1-213-740-6952; ellis.meng@usc.edu